

ChemComm

Accepted Manuscript



This article can be cited before page numbers have been issued, to do this please use: N. Kameta and H. Shiroishi, *Chem. Commun.*, 2018, DOI: 10.1039/C8CC02013B.



This is an Accepted Manuscript, which has been through the Royal Society of Chemistry peer review process and has been accepted for publication.

Accepted Manuscripts are published online shortly after acceptance, before technical editing, formatting and proof reading. Using this free service, authors can make their results available to the community, in citable form, before we publish the edited article. We will replace this Accepted Manuscript with the edited and formatted Advance Article as soon as it is available.

You can find more information about Accepted Manuscripts in the [author guidelines](#).

Please note that technical editing may introduce minor changes to the text and/or graphics, which may alter content. The journal's standard [Terms & Conditions](#) and the ethical guidelines, outlined in our [author and reviewer resource centre](#), still apply. In no event shall the Royal Society of Chemistry be held responsible for any errors or omissions in this Accepted Manuscript or any consequences arising from the use of any information it contains.

COMMUNICATION

PEG-nanotube liquid crystals as templates for construction of surfactant-free gold nanorods

Cite this: DOI: 10.1039/x0xx00000x

Naohiro Kameta^{a*} and Hidenobu Shiroishi^bReceived 00th March 2018,
Accepted 00th March 2018

DOI: 10.1039/x0xx00000x

www.rsc.org/

Lyotropic liquid crystals, in which nanotubes coated with polyethylene glycol were aligned side-by-side in aqueous dispersions, acted as templates for the construction of surfactant-free gold nanorods with controllable diameters, functionalizable surfaces, and tunable optical properties.

Gold nanorods (GNRs) are attractive materials for basic research and technological applications because of the unique optical properties that arise from their morphological anisotropy. For example, the localized surface plasmon resonance (LSPR) and photothermal properties exhibited by GNRs are widely utilized for sensing and imaging, drug delivery, photothermal therapy, catalysis, and solar cells.¹ GNRs are generally produced by chemical reduction of gold ions in surfactant solutions. The surfactants are indispensable for achieving one-dimensional growth of the crystal nucleus; in the absence of surfactants, morphologically isotropic spherical and plate-like structures are obtained.² However, GNRs produced in surfactants are covered with dense layers of surfactant molecules, which often are highly cytotoxic and which prevent chemical modification of the GNRs.³

Various alternatives to surfactants have been investigated as templates for the construction of metal/inorganic nanostructures, including GNRs. Previously reported alternatives include nanoporous materials such as polycarbonate and alumina membranes,⁴ as well as organic nanotubes⁵ formed by self-assembly of amphiphilic molecules.⁶ However, such template methods present some problems. For example, the GNRs obtained by template methods tend to have structural defects resulting from the low efficiencies with which the starting agents are loaded into the nanochannels of the templates; and the isolated yields of GNRs are low because the templates are difficult to remove and separate.

Herein we describe the use of lyotropic liquid crystals, consisting of organic nanotubes coated with hydrated polyethylene glycol (PEG) and aligned side-by-side, as templates to construct surfactant-free GNRs. This template method enabled us not only to tune the diameters and LSPR properties of the GNRs but also to densely functionalize the GNR surface with thiol-crown ether compounds. The thiol-functionalized GNRs exhibited selective ion recognition and chiral molecular recognition.

As previously reported,⁷ self-assembly of glycolipid-based amphiphiles with a hydrophilic D-glucose headgroup at one end and a different hydrophilic headgroup at the other end produces molecular monolayer nanotubes. In this study, we synthesized amphiphiles **1(n)** and PEG derivatives **2(n)**, where $n = 2, 6, \text{ and } 10$ (Fig. 1a), and carried out binary self-assembly of **1(n)** and **2(n)** with identical n values by refluxing stoichiometric mixtures of **1(n)** and **2(n)** in pure water and then gradually cooling the reaction mixtures to room temperature (see ESI for experimental details). Transmission electron microscopy (TEM) revealed that this process

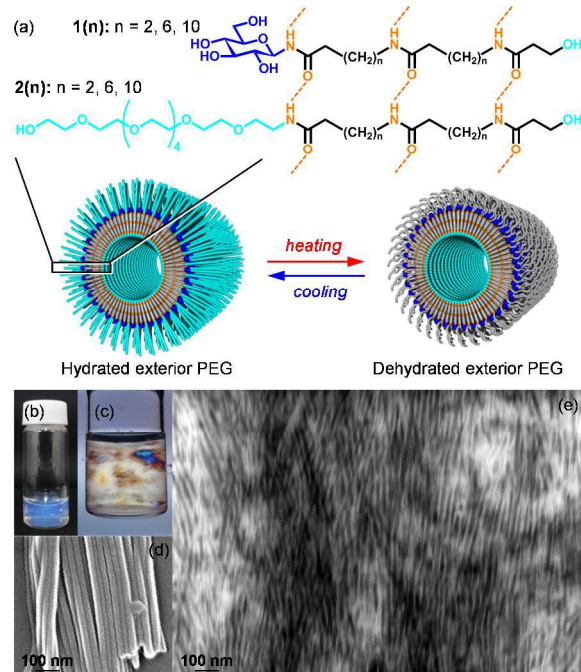


Fig. 1 (a) Schematic representation of PEG nanotubes formed by binary self-assembly of **1(n)** and **2(n)** and subsequent thermal dehydration and rehydration of the exterior PEG chains. (b, c) Photographs of NT-LCs composed of **1(2)** and **2(2)** obtained without (b) and with (c) a cross polarizer. (d) SEM and (e) TEM images of side-by-side aligned nanotubes in dry-state NT-LCs.

gave only nanotubes, whereas self-assembly of single-component dispersions of **2(2)**, **2(6)**, and **2(10)** formed micelles, nanofibers, and sheets, respectively (Fig. S1, ESI). The differential scanning calorimetry profile of each of the three types of nanotubes showed an endothermic peak corresponding to an isotropic melting point that was different from the melting points of the corresponding assemblies of **1(n)** alone or **2(n)** alone (Fig. S2, ESI). These results confirmed that the nanotubes were composed of **1(n)** and **2(n)**.

Powder X-ray diffraction and infrared spectroscopy revealed that the nanotubes consisted of a monolayer membrane in which **1(n)** and **2(n)** were packed parallel to each other, as indicated by the presence of intermolecular hydrogen bonding between the amide moieties, as well as by hydrophobic and van der Waals interactions between the oligomethylene chains (Fig. S3, ESI). The thicknesses of the membrane walls of the nanotubes were estimated from TEM images to be approximately 5–7 nm (Fig. S1, ESI), a range that is comparable to the extended molecular lengths (L) of **2(n)**: 4.82, 5.78, and 6.74 nm for $n = 2, 6,$ and 10 , respectively. The inner diameters (i.d.) of the nanotubes were uniform and increased with increasing L : i.d. = 18, 23, and 31 nm for $n = 2, 6,$ and 10 , respectively. For nanotubes with monolayer membranes composed of asymmetric amphiphiles, the i.d. can sometimes be calculated using the following equation: $\text{i.d.} = 2a_2L/(a_1 - a_2)$, where a_2 and a_1 are the cross-sectional areas of the small and large headgroups, respectively.⁷ That is, i.d. is proportional to L if a_2 and a_1 are constant. Elongation of the oligomethylene chain theoretically increases the i.d. by 6 nm for every eight methylene units. Although the experimentally observed increment in the i.d. values in this study was more irregular than predicted by the above-mentioned equation, the trend we observed was in accordance with the equation. The parallel molecular packing of **1(n)** and **2(n)** induced curvature of the monolayer membrane, owing to the size difference between the D-glucose headgroup (or the PEG moiety) and the hydroxyl headgroup, the former two being larger than the latter. The large headgroups and the small headgroups must be located on the outer and inner surfaces of the nanotubes, respectively (Fig. 1a).

The nanotubes prepared as described above had lengths of several micrometers. Sonication of the nanotubes shortened their lengths and enhanced their dispersibility in water. The length distributions of the shortened nanotubes were estimated from TEM images, and the peaks of the distributions were around 400–600 nm (Fig. S4, ESI). The visual appearance of aqueous dispersions of the nanotubes was remarkably influenced by nanotube concentration (Fig. S5, ESI). When the concentration was <0.2 wt%, the dispersions were clear, whereas when the concentration was in the 0.2–5 wt% range, the dispersions were bluish, owing to Rayleigh

scattering (Fig. 1b). Birefringence was also observed under a cross polarizer (Fig. 1c), indicating formation of lyotropic liquid crystals.^{7,8} Scanning electron microscopy (SEM) and TEM of the liquid crystals in the dry state showed side-by-side alignment of the nanotubes (Fig. 1d,e). In contrast, the nanotubes were found to be oriented randomly in the clear aqueous dispersions obtained at concentrations of <0.2 wt%, and networked structures of nanotubes were observed in the hydrogels that were obtained at concentrations of >5 wt%. The nanotube liquid crystals (hereafter abbreviated as NT-LCs) are assignable to a nematic type.

The NT-LCs were stable at room temperature, but they broke apart at elevated temperatures; and, as a result, the nanotubes formed aggregates and precipitated from the aqueous solutions. This phenomenon is ascribable to dehydration of the PEG chains on the outer surface of the nanotubes, as indicated by changes in the C–C bonds from the gauche conformation at low temperatures to the anti conformation at high temperatures.⁹ Lowering the temperature resulted in rehydration of the PEG chains. The dehydration and rehydration temperatures (T_{-H_2O} and T_{+H_2O}) of the PEG chains were 55–60 and 40–45 °C, respectively, as determined by means of turbidity measurements (Fig. S6, ESI). The appearance/disappearance cycle for the NT-LCs—that is, the dispersion/aggregation cycle of the nanotubes that occurred as a result of thermal dehydration/rehydration of the PEG chains—could be repeated several times. This unique behavior was useful for separation of these nanotube templates from GNRs prepared as described in the next paragraph.

The NT-LCs were used as templates for the production of surfactant-free GNRs (see ESI for experimental details). First, we added 3.5-nm gold seed particles¹⁰ to the NT-LCs (Fig. 2a). TEM clearly showed one-dimensional alignment of the seed particles on the surfaces of the side-by-side aligned nanotubes (Fig. 3a). The seed particles did not become encapsulated in the nanotube channels under these conditions, because encapsulation would have required capillary action or some specific interaction between the seed particles and the nanotube channels.^{6b} We expected that the seed particles would be trapped in grooves between the nanotubes comprising the NT-LCs (Fig. 2b), and in fact seed particles were observed only in the grooves and not around isolated nanotubes or at the ends of the aligned nanotubes (Fig. 3a). Second, we treated the NT-LCs with a growth solution containing HAuCl₄ and ascorbic acid as a weak reducing agent, and the result was the formation of GNRs with uniform diameters (Figs. 2c,d and 3b). Growth solutions usually include surfactants such as cetyltrimethylammonium bromide



Fig. 2 Production of GNRs using NT-LC templates.

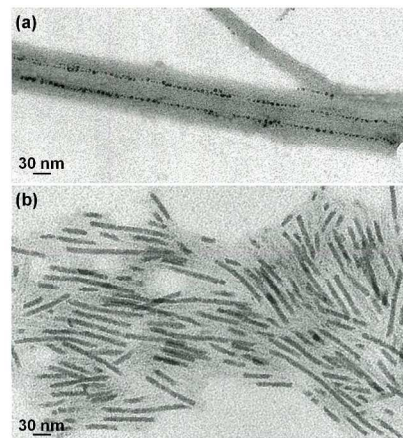


Fig. 3 (a) TEM image of one-dimensional alignments of gold seed particles trapped in the grooves between side-by-side aligned nanotubes in a NT-LC template composed of **1(2)** and **2(2)**. (b) TEM image of GNRs grown from the gold seed particles on the NT-LC template.

(CTAB), which are required to obtain GNRs with anisotropic morphology and controllable diameters. However, in the present system, the monolayer membrane walls of the nanotubes assumed the role played by CTAB micelles or bilayer membranes. We found that when nanotube hydrogels consisting of networked structures of randomly oriented nanotubes were used in this procedure in place of the NT-LCs, we obtained gold nanoparticles instead of GNRs (Fig. S7, ESI); and nanoparticles also formed in the absence of the nanotube hydrogels and in the absence of CTAB (data not shown). These results suggest that the grooves formed by the side-by-side aligned nanotubes in the NT-LCs were necessary not only for entrapment of the seed particles but also for growth of the entrapped particles into GNRs.

When thiol-crown ether compounds were present in the system, thermal dehydration of the PEG chains on the outer surface of the nanotubes induced nanotube aggregation and spontaneous release of thiol-functionalized GNRs (Fig. 2e–g). We found that the photothermal effect induced by near-infrared irradiation (Nd-YAG laser, 1064 nm, 0.7 W) was more effective than general direct

heating of the entire system at temperatures above T_{-H_2O} (= 55–60 °C). The use of near-infrared irradiation led to complete recovery of the GNRs, whereas direct heating left almost all of the GNRs in the NT-LC templates (Fig. S8, ESI). The temperature during near-infrared irradiation was estimated to be 42 °C, which was lower than T_{-H_2O} . We attributed the initiation of PEG chain dehydration to localized heating via a photothermal effect of the GNRs, which were in close contact with the nanotubes, because we confirmed that irradiation of the NT-LCs under the same conditions but in the absence of the GNRs failed to induce NT-LC destruction and nanotube aggregation.

The diameters and lengths of the isolated thiol-functionalized GNRs were estimated from SEM and TEM images (Fig. 4a; Fig. S9, ESI) and were plotted against the outer diameters (i.d. + membrane thickness) of the nanotubes in the NT-LC templates (Fig. 4b,c). GNR diameter was found to be proportional to nanotube outer diameter, a result that supports our conclusion that GNR growth occurred only in the grooves between the aligned nanotubes in the NT-LC templates (Fig. 3d). The GNR diameters were reasonably consistent with the size of the grooves, which increased with increasing nanotube outer diameter (Fig. 4e). In contrast, GNR length was independent of nanotube outer diameter (Fig. 4c) and was also unrelated to nanotube length (400–600 nm, Fig. S4, ESI). Absorption spectroscopy revealed that the GNRs exhibited LSPR bands in the visible and near-infrared regions (Fig. 4d). The absorption intensity in the visible region and the maximum absorption wavelength in the near-infrared region reflected the aspect ratio (= length/diameter) of the GNRs. Our results were consistent with the generally observed trend that higher aspect ratios result in a less intense absorbance in the visible region and a longer maximum absorption wavelength.¹¹ The present template method enabled us to produce GNRs with tunable optical features.

After removal of the NT-LC templates by near-infrared irradiation, the GNRs functionalized with thiol-12-crown-4 ether compound **3** or thiol-15-crown-5 ether compound **4** (hereafter abbreviated as 12crown4-GNRs and 15crown5-GNRs) were

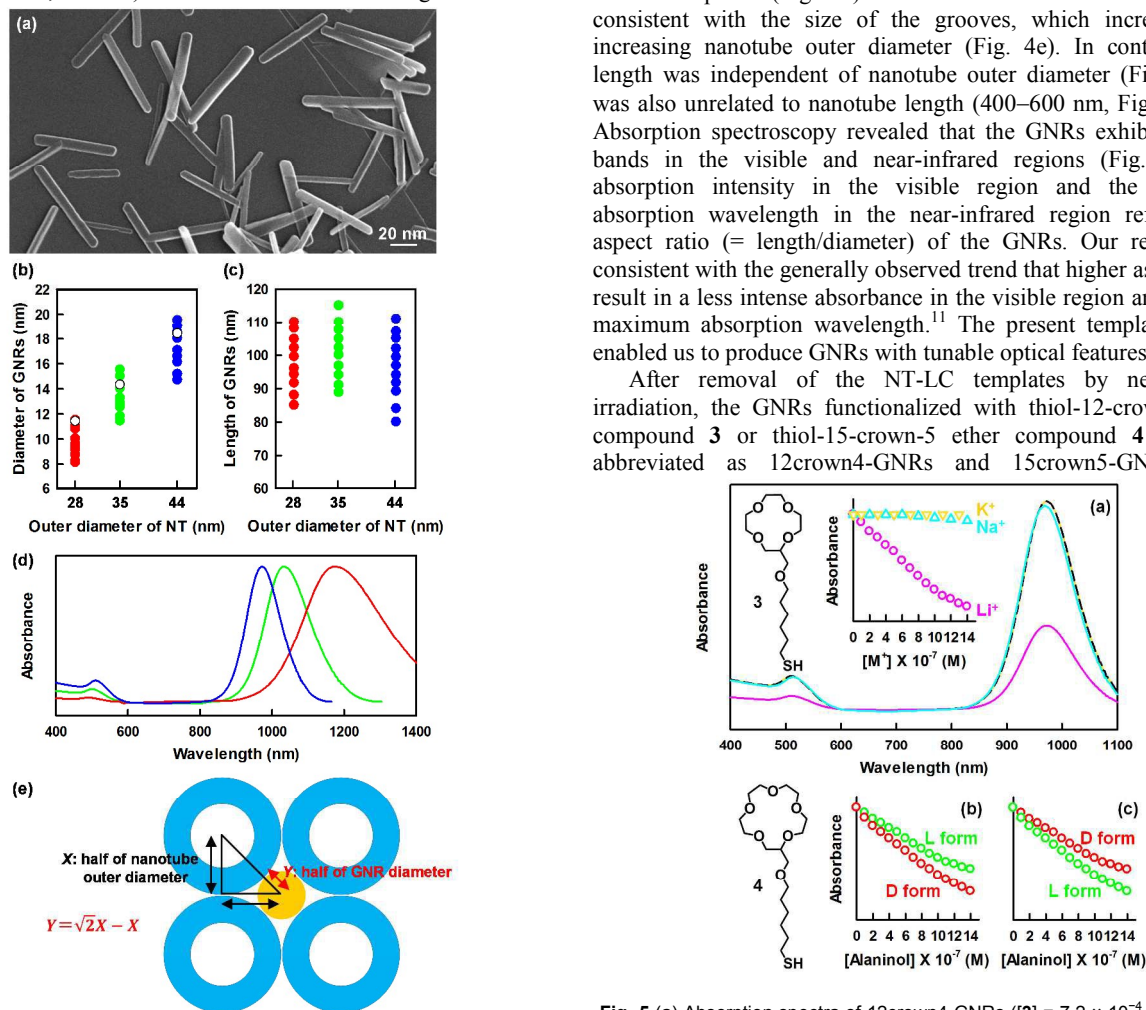


Fig. 4 (a) SEM image of thiol-functionalized GNRs (12crown4-GNRs) separated from a NT-LC template composed of **1(2)** and **2(2)**. (b, c) Plots of 12crown4-GNR diameters (b) and lengths (c) against the outer diameters of the nanotubes in the NT-LC templates. Solid symbols indicate experimental values estimated from SEM and TEM images, and open symbols indicate values calculated by using the equation in panel (e). (d) Absorption spectra of aqueous dispersions of 12crown4-GNRs; the colors correspond to the colors in panels (b) and (c). (e) Schematic representation of the relationship between GNR diameter and nanotube diameter.

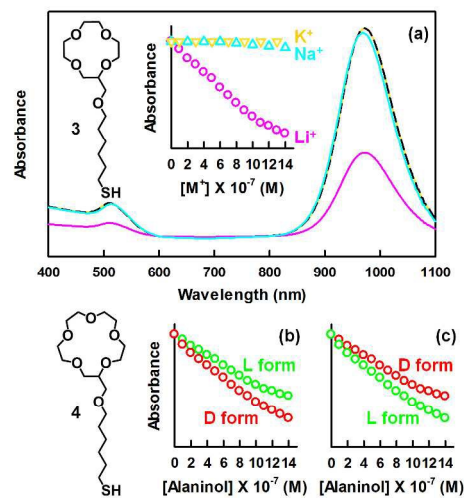


Fig. 5 (a) Absorption spectra of 12crown4-GNRs ($[3] = 7.2 \times 10^{-4}$ M) in water in the absence and presence of 1.4×10^{-6} M Li⁺ (pink), Na⁺ (blue), and K⁺ (yellow). Inset: Plot of absorbance at 970 nm versus initial ion concentration. The 12crown4-GNRs were prepared by using a NT-LC template composed of **1(10)** and **2(10)**. The diameters and lengths of the 12crown4-GNRs are shown in blue in Fig. 4b,c. (b, c) Plots of absorbance at 970 nm of 15crown5-GNRs ($[4] = 6.5 \times 10^{-4}$ M) versus initial concentration of D- and L-alaninols. The 15crown5-GNRs in panel (b) were prepared by using a NT-LC template composed of **1(10)** with a D-glucose headgroup and **2(10)**, and the GNRs in panel (c) were prepared by using a template composed of an enantiomer (with an L-glucose headgroup) of **1(10)** and **2(10)**.

investigated for molecular recognition of alkaline metal ions and chiral amines, respectively. Upon addition of Li ions to an aqueous dispersion of 12crown4-GNRs led to a decrease in the intensities of the LSPR bands but no shift in the peak wavelengths (Fig. 5a). The lack of peak shifts indicates that the 12crown4-GNRs did not undergo aggregation. The decrease in peak intensity is attributable to a 1:1 host-guest interaction between the Li ions and the 12-crown-4 ether moieties on the surface of the 12crown4-GNRs. In contrast, the LSPR bands showed no response to the addition of Na or K ions, despite the fact that the formation of sandwich-type 2:1 host-guest complexes between 12-crown-4 ether and Na and K ions is known to occur. GNRs functionalized with **3** by means of a ligand-exchange reaction of CTAB-coated GNRs are reported to form aggregates with Na and K ions by means of a sandwich-type 2:1 host-guest interaction.¹² The Li-ion selectivity observed for the present 12crown4-GNRs was attributed to the direct functionalization of the surfactant-free GNRs with **3**. The 12-crown-4 ether moieties densely functionalized on the 12crown4-GNRs prohibited sandwich-type 2:1 host-guest interactions with Na and K ions (Fig. S10, ESI).

Addition of D- or L-alaninol to an aqueous dispersion of 15crown5-GNRs led to decreases in the intensities of the LSPR bands but no shifts in the peak wavelengths (Fig. 5b). The decrease was larger for D-alaninol than for L-alaninol, indicating that the 15crown5-GNRs exhibited chiral recognition ability. In contrast, 15crown5-GNRs, which are prepared from a NT-LC template containing an enantiomer (with a L-glucose headgroup) of **1(n)**, showed higher affinity for L-alaninol (Fig. 5c). To obtain chiral information of the GNRs, we conjugated pyrene acting as a VIS absorption marker to the two 15crown5-GNRs. Both GNRs each other have positive/negative symmetrical Cotton bands at the absorption wavelength of the pyrene moieties anchored to the most outer surface through the alkyl chain and crown ether, even though the pyrene-15crown5 itself is achiral (Fig. S11, ESI). This indicates that the supramolecular chirality of the NT-LC templates is conferred and transcribed to the surface of the GNRs. The induction of chirality in polymers encapsulated in nanotube channels and nanoparticles adsorbed on the nanotube outer surface with supramolecular chirality has previously been reported.^{7, 13} However, the present study is the first to indicate that grooves shaped by the outer surfaces of side-by-side aligned nanotubes can act as chirality inducers and, furthermore, that the induced chirality of 15crown5-GNRs generated in the grooves was retained after separation of the GNRs from the NT-LC templates.

In conclusion, we constructed surfactant-free GNRs with controllable diameters and tunable optical properties by using NT-LCs as templates. GNRs densely functionalized with thiol-crown ethers exhibited highly selective ion recognition and chiral recognition abilities. The present method is superior not only to previously reported template methods using nanochannels of nanoporous materials and nanotubes but also to conventional ligand-exchange methods involving GNRs precoated with surfactants, in terms of the dimensional control, isolation, and functionalization efficiency. Precise design of NT-LC templates can be expected to facilitate the use of GNRs for various applications, including as sensors, drugs, and catalysts.

This work was supported by a KAKENHI from the Japan Society for the Promotion of Science (grant no. JP17H02726).

Notes and references

^a Nanomaterials Research Institute, Department of Materials and Chemistry, National Institute of Advanced Industrial Science and Technology (AIST), Tsukuba Central 5, 1-1-1 Higashi, Tsukuba, Ibaraki 305-8565, Japan.

E-mail: n-kameta@aist.go.jp; Fax: +81-29-861-4545; Tel: +81-29-861-4478

^b National Institute of Technology, Tokyo College, Kunugida 1220-2, Hachioji, Tokyo, 193-0997, Japan.

† Electronic Supplementary Information (ESI) available: Synthesis of **1(n)**, **2(n)**, **3** and **4**; self-assembly procedure; TEM, molecular packing analysis, and length distributions of the nanotubes; pictures of nanotube hydrogels; determination of T_{-H_2O} and T_{+H_2O} ; production procedure of gold seed particles and GNRs; TEM images of GNRs and gold nanoparticles; release profiles of GNRs from NT-LCs; schematic images of molecular recognition; circular dichroism spectra of GNRs. See DOI: 10.1039/c800000x/

- (a) N. D. Burrows, W. Lin, J. G. Hinman, J. M. Dennison, A. M. Vartanian, N. S. Abadeer, E. M. Grzincic, L. M. Jacob, J. Li, C. J. Murphy, *Langmuir*, 2016, **32**, 9905; (b) S. Jayabal, A. Pandikumar, H. N. Lim, R. Ramaraj, T. Sun, N. M. Huang, *Analyst*, 2015, **140**, 2540; (c) W. I. Choi, A. Sahu, Y. H. Kim, G. Tae, *Ann. Biomed. Eng.*, 2012, **40**, 534.
- (a) J. G. Hinman, A. J. Stork, J. A. Varnell, A. A. Gewirth, C. J. Murphy, *Faraday Discuss.*, 2016, **191**, 9; (b) Y. Takenaka, Y. Kawabata, H. Kitahata, M. Yoshida, Y. Matsuzawa, T. Ohzono, *J. Colloid Interface Sci.*, 2013, **407**, 265 (2013); (c) Y.-Y. Yu, S.-S. Chang, C.-L. Lee, C. R. C. Wang, *J. Phys. Chem. B*, 1997, **101**, 6661.
- (a) B. Thierry, J. Ng, T. Krieg, H. J. Griesser, *Chem. Commun.*, 2009, **45**, 1724; (b) T. Niidome, M. Yamagata, Y. Okamoto, Y. Akiyama, H. Takahashi, T. Kawano, Y. Katayama, Y. Niidome, *J. Control. Release*, 2006, **114**, 343.
- (a) J. Cao, T. Son, K. T. V. Grattan, *Sens. Actuators B Chem.*, 2014, **195**, 332; (b) L. Vigderman, B. P. Khanal, E. R. Zubarev, *Adv. Mater.*, 2012, **24**, 4811.
- (a) T. Shimizu, *Bull. Chem. Soc. Jpn.*, 2018, **91**, 623; (b) R. L. Beingessner, Y. Fana, H. Fenniri, *RSC Adv.*, 2016, **6**, 75820; (c) Y. Kim, W. Li, S. Shin, M. Lee, *ACC. Chem. Res.*, 2013, **46**, 2888; (d) T. Aida, E. W. Meijer, S. I. Stupp, *Science*, 2012, **335**, 813.
- (a) L. Adler-Abramovich, E. Gazit, *Chem. Soc. Rev.*, 2014, **43**, 6881; (b) T. Shimizu, H. Minamikawa, M. Kogiso, M. Aoyagi, N. Kameta, W. Ding, M. Masuda, *Polym. J.*, 2014, **46**, 831; (c) J. H. Jung, M. Park, S. Shinkai, *Chem. Soc. Rev.*, 2010, **39**, 4286.
- T. Shimizu, N. Kameta, W. Ding, M. Masuda, *Langmuir*, 2016, **32**, 12242.
- P. Terech, B. Jean, F. Ne, *Adv. Mater.*, 2006, **18**, 1571.
- (a) M. J. Hey, S. M. Ilett, G. Davidson, *J. Chem. Soc. Faraday Trans.*, 1995, **91**, 3897; (b) M. Björling, G. Karlström, P. Linse, *J. Phys. Chem.*, 1991, **95**, 6706.
- B. D. Busbee, S. O. Obare, C. J. Murphy, *Adv. Mater.*, 2003, **15**, 414.
- S. Link, M. B. Mohamed, M. A. El-Sayed, *J. Phys. Chem. B.*, 1999, **103**, 3073
- H. Nakashima, K. Furukawa, Y. Kashimura, K. Torimitsu, *Chem. Commun.*, 2007, **43**, 1080.
- (a) J. Cheng, G. L. Saux, J. Gao, T. Buffeteau, Y. Battie, P. Barois, V. Ponsinet, M.-H. Delville, O. Ersen, E. Pouget, R. Oda, *ACS Nano*, 2017, **11**, 3806; (b) M. Numata, S. Shinkai, *Chem. Commun.*, 2011, **47**, 1961.

Graphical Table of Contents

PEG-nanotube liquid crystals as templates for construction of surfactant-free gold nanorods

Naohiro Kameta,* and Hidenobu Shiroishi

Nanogrooves shaped by side-by-side alignment of PEG nanotubes in water precisely assisted growth of gold seeds to nanorods without surfactants.

